Available online at www.sciencedirect.com
ScienceDirect
Applied Thermal Engineering 28 (2008) 1251–1258
APPLIED THERMAL ENGINEERING
www.elsevier.com/locate/apthermeng

Numerical analysis of heat transfer in a passive solar composite wall with porous absorber

Wei Chen [a,*], Wei Liu [b]

[a] School of Merchant Marine, Shanghai Maritime University, Shanghai 200135, PR China
[b] School of Energy and Power Engineering, Huazhong University of Science and Technology, Wuhan 430074, PR China

Received 18 March 2007; accepted 24 October 2007
Available online 30 October 2007

Abstract

In this paper, heat transfer and flow in the two types of composite solar wall with porous absorber has been studied. The 'unsteady' numerical simulation is employed to analyze the performance of the flow and temperature field in the composite solar wall. The excess heat is stored within the porous absorber during solar radiation and there is stratification in the porous layer. So, the porous absorber works as thermal insulator in a degree when no solar shining is available. The heating characteristic of the two types of the composite solar wall with porous absorber has been analyzed. The influence of the particle size, the porosity, the thermal conductivity of porous layer and the porous absorber position in the solar composite wall on the air temperature in the heated room is significant. The results show that all these factors should be taken into account for a better design of the heating system.

Keywords: Porous absorber; Solar energy; Heat transfer

1. Introduction

Passive solar heating is widely used in the cold climates. The storage walls have been extensive use since the works of Trombe [1,2] were published. The standard Trombe wall has the drawback of low thermal resistance, which leads to significant losses at night-time or during periods with no sun. Furthermore, part of the heat supply cannot be controlled (risk of overheating). A composite solar wall enables these drawbacks to be overcome. The composite collector system was studied [3], which consists of a glazing wall, a massive wall and an insulating wall; there is a convective channel between the massive wall and the insulating wall, and no convective channel locates between the massive wall and the glazing. The composite collector system with porous absorber was also conceived and studied. A porous wall is used between the glazing and the massive wall [4,5] or a non-convective porous wall [6]. In these cases, the absorbed solar radiation is transmitted to the heated room by conduction and convection, the characteristics of non-convective porous wall should be analyzed further.

In this study, the two kinds of composite wall with convective porous absorber shown schematically in Fig. 1 have been investigated. The numerical simulation was carried out to analyze the variation of the flow and the temperature field in the composite solar wall and the effects of the particle size and the porosity within the porous layer, the thermal conductivity of porous layer and the porous absorber position in the solar composite wall on the heating. Major objective of the present study focuses on the selecting efficient strategies for the composite solar wall system with porous absorber of the heating building.

2. System description and mathematical analysis

2.1. System description

The two kinds of passive solar composite wall with porous absorber under investigation are schematically shown

* Corresponding author. Tel.: +86 21 58855200x2120.
E-mail address: weichen96@sina.com (W. Chen).

1359-4311/$ - see front matter © 2007 Elsevier Ltd. All rights reserved.
doi:10.1016/j.applthermaleng.2007.10.017

Nomenclature

A	area (m^2)
c	specific heat (J/(kg K))
C	inertia coefficient (see Eq. (10))
d	diameter (m)
g	gravitational acceleration vector (m/s^2)
G_{sun}	rate of solar flux incident on the glass cover (W/m^2)
h_{po}	horizontal coordinate of the outside surface of the porous absorber (m)
h_{pi}	horizontal coordinate of the inside surface of the porous absorber (m)
h_{wi}	convection heat transfer coefficient between the air in the heated room and the inside surface of the thermal storage wall ($W/(m^2\ K)$)
k	thermal conductivity (W/(m K))
k_f	fluid thermal conductivity (W/(m K))
k_m	apparent thermal conductivity (W/(m K))
k_s	solid thermal conductivity (W/(m K))
k_w	thermal conductivity of thermal storage wall (W/(m K))
K	permeability of porous medial (m^2)
p	pressure (Pa)
Q_{apo}	convective heat exchange between the air and the outside surface of the porous absorber (J)
Q_{api}	convective heat exchange between the air and the inside surface of the porous absorber (J)
Q_{cai}	convective heat exchange between the air and the inside surface of the glass cover (J)
Q_{cao}	convective heat exchange between the ambient air and the outside surface of the glass cover (J)
Q_{gp}	thermal radiation exchange between the glass enclosure and the surface of porous absorber (J)
Q_{gsky}	thermal radiation exchange between the glass enclosure and sky (J)
Q_{pw}	thermal radiation exchange between the surface of thermal storage wall and the porous absorber surface (J)
Q_{wr}	heat exchange between the air in the heated room and the enclosure except the surface of thermal storage wall (J)
T	temperature (K (°C))
T_{ao}	ambient temperature (°C)
T_{room}	air temperature in the heated room (K (°C))
u	velocity component in x-direction (m/s)
$\lvert\vec{v}_d\rvert$	mean velocity $\left(=\sqrt{u_d^2+v_d^2}\right)$ (m/s)
v	velocity component in y-direction (m/s)
V	volume of heated room (m^3)
x	horizontal coordinate (m)
y	vertical coordinate (m)

Greek symbols

β	thermal expansion coefficient (1/K)
τ	time (s)
Γ	exchange coefficient
μ	dynamic viscosity (kg/(m s))
ρ	density (kg/m^3)
θ	porosity of the porous medium
η_g	absorptivity of the glass cover
η_p	absorptivity of the porous absorber outside surface
δ	transmissivity of the glass cover

Subscripts

c	cold wall
d	Darcy
eff	effective
f	fluid
m	apparent mean
p	porous medial
room	heated room
s	solid of porous absorber
wall	thermal storage massive wall

Superscripts

−	average
+	on the right side of the horizontal coordinate position
–	on the left side of the horizontal coordinate position

in Fig. 1a and b. The composite wall locates on the south side of the heated room and consists of a glazing, a massive thermal storage wall and a porous layer that is used between the glazing and the massive thermal storage wall. There is an air gap between the glazing and the porous layer. The composite wall system in which the porous layer adheres with massive thermal storage wall is contact type, shown in Fig. 1a. In contrast, there is an air channel between the porous layer and the massive thermal storage wall, which has a top and a bottom vent to facilitate the convection, is called separation type shown in Fig. 1b.

The porous layer is heated by solar radiation. A part of solar energy is absorbed and stored in the porous layer, the rest energy transmitted through the porous layer is available to increase the air temperature in the heated room and stored in the massive thermal storage wall.

2.2. Theoretical modeling

The flow is assumed to be laminar and two-dimensional. The Boussinesq approximation is used to account for the

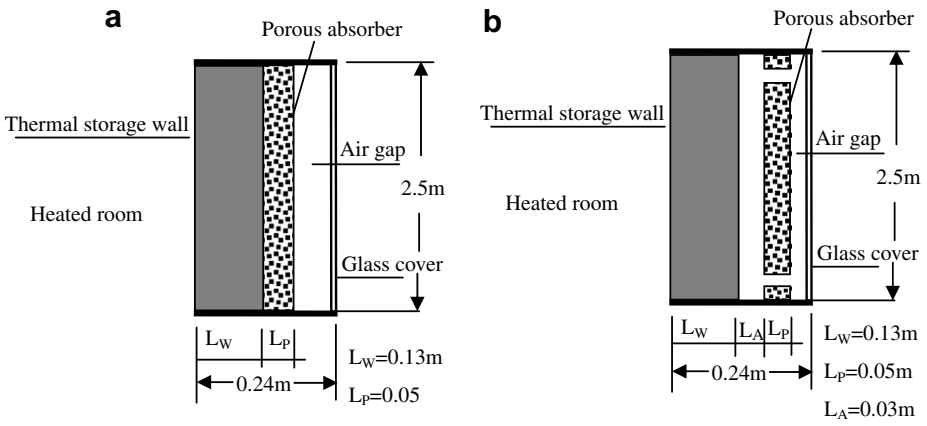

Fig. 1. Schematic of a passive solar composite wall with porous absorber: (a) contact type passive solar composite wall with porous absorber and (b) separation type passive solar composite wall with porous absorber.

density variation. While the flow in the composite wall except the porous absorber is governed by the Navier–Stokes equations, flow in the porous absorber is governed by Brinkman–ForchHeimer Extended Darcy model [7]. The mathematical model is described below:

For the flow in the composite wall (except the convective porous layer), the governing equations can be written as

Continuity equations

$$\frac{\partial(\rho u)}{\partial x}+\frac{\partial(\rho v)}{\partial y}=0 \tag{1}$$

Momentum equations

$$\frac{\partial(\rho u)}{\partial \tau}+\frac{\partial(\rho u u)}{\partial x}+\frac{\partial(\rho v u)}{\partial y} =-\frac{\partial p}{\partial x}+\frac{\partial}{\partial x}\left(\mu\frac{\partial u}{\partial x}\right)+\frac{\partial}{\partial y}\left(\mu\frac{\partial u}{\partial y}\right) \tag{2}$$

$$\frac{\partial(\rho v)}{\partial \tau}+\frac{\partial(\rho u v)}{\partial x}+\frac{\partial(\rho v v)}{\partial y} =-\frac{\partial p}{\partial y}+\frac{\partial}{\partial x}\left(\mu\frac{\partial v}{\partial x}\right)+\frac{\partial}{\partial y}\left(\mu\frac{\partial v}{\partial y}\right)+\rho g\beta(T-T_C) \tag{3}$$

Energy equation

$$\rho c\frac{\partial T}{\partial \tau}+\rho c\left(u\frac{\partial T}{\partial x}+v\frac{\partial T}{\partial y}\right)=\frac{\partial}{\partial x}\left(k\frac{\partial T}{\partial x}\right)+\frac{\partial}{\partial y}\left(k\frac{\partial T}{\partial y}\right) \tag{4}$$

For flow and heat transfer in the convective porous layer, the governing equations can be written as

Continuity equation

$$\frac{\partial(\rho u_d)}{\partial x}+\frac{\partial(\rho v_d)}{\partial y}=0 \tag{5}$$

Momentum equations

$$\frac{\rho}{\theta}\frac{\partial u_d}{\partial \tau}+\frac{\rho}{\theta}\left(u_d\frac{\partial u_d}{\partial x}+v_d\frac{\partial u_d}{\partial y}\right) =-\frac{\partial p}{\partial x}+\frac{\partial}{\partial x}\left(\mu_{\text{eff}}\frac{\partial u_d}{\partial x}\right)+\frac{\partial}{\partial y}\left(\mu_{\text{eff}}\frac{\partial u_d}{\partial y}\right) -\frac{\mu u_d}{K}+\frac{\rho C\theta}{\sqrt{K}}|\vec{v}_d|u_d \tag{6}$$

$$\frac{\rho}{\theta}\frac{\partial v_d}{\partial \tau}+\frac{\rho}{\theta}\left(u_d\frac{\partial v_d}{\partial x}+v_d\frac{\partial v_d}{\partial y}\right) =-\frac{\partial p}{\partial y}+\frac{\partial}{\partial x}\left(\mu_{\text{eff}}\frac{\partial v_d}{\partial x}\right)+\frac{\partial}{\partial y}\left(\mu_{\text{eff}}\frac{\partial v_d}{\partial y}\right) -\frac{\mu v_d}{K}+\frac{\rho C\theta}{\sqrt{K}}|\vec{v}_d|v_d+\rho g\beta(T-T_c) \tag{7}$$

Energy equation

$$(\rho c)_m\frac{\partial T}{\partial \tau}+\rho c\left(u_d\frac{\partial T}{\partial x}+v_d\frac{\partial T}{\partial y}\right) =\frac{\partial}{\partial x}\left(k_{\text{eff}}\frac{\partial T}{\partial x}\right)+\frac{\partial}{\partial y}\left(k_{\text{eff}}\frac{\partial T}{\partial y}\right) \tag{8}$$

where all constants and variables are defined in the nomenclature, Eqs. (5)–(8) form the full set of equations used to model convective flows in porous media. Eqs. (6) and (7) contain the usual balance of forces between viscosity and pressure gradient known as Darcy's law (viz. the 3rd and 6th terms), which are extended by the further inclusion of terms modeling in turn advective inertia (1st and 2nd terms), boundary effects (the 4th and 5th terms: the Brinkman term) and form-drag (Forchheimer inertia, the 6th term). Eq. (7) contains buoyancy (the 8th term). The values for the permeability K and the inertia coefficient C in the momentum equations for the porous layer are given by Ergun (1952) [8,9]. For the porous layer of particle diameters d_p and porosity θ.

$$K=\frac{d_p^2\theta^3}{175(1-\theta)^2} \tag{9}$$

$$C=\frac{1.75}{\sqrt{175}}\theta^{-3/2} \tag{10}$$

In addition, models for the effective properties (μ_{eff} and k_m) of the porous medium are needed. It has been found that taking $\mu_{eff} = \mu_f$ in Brinkman's extension provides good agreement with experimental data (Neale and Nader, 1974) [10] and is adopted in the present work. In present study, the conductivity of the medium k_m and $(\rho c)_m$ is calculated as following: $k_m = \theta k_f + (1-\theta)k_s$, $(\rho c)_m = \theta(\rho c)_f + (1-\theta)(\rho\ c)_s$ [11].

2.3. Boundary conditions and initial conditions

Numerical simulations were performed for sunny and control based on air temperature and operative conditions was considered. A typical cold day was considered for Shanghai, China in November with the outdoor temperature [12] and solar irradiance variation [13] given by Eqs. (11) and (12).

$$T_{ao}(\tau) = \overline{T_{ao}} + T_{ar}\cos\left(\frac{\pi}{12}(\tau - 14)\right) \tag{11}$$

$$G_{sun}(\tau) = \hat{G}_{sun}\sin\left(\frac{\tau - a}{b - a}\pi\right), \quad a < \tau < b \tag{12}$$

where $\overline{T_{ao}}$ is the average outside temperature of 15 °C; T_{ar} is amplitude of 6 °C; $\hat{G}_{sun}$ is maximum solar irradiance of 400 W/m^2; a is sunrise hour of 6 o'clock in the morning; b is the sunset hour of 18 o'clock in the afternoon; τ: time, hours.

The fluid in the solar heating system is initially stagnant and at a uniform temperature which is the same as the ambient temperature. In terms of mathematical expressions, the initial and boundary conditions drawn from energy-balance equations are given below:

For the glass cover of the composite wall

$$\eta_g G_{sun} + Q_{gsky} + Q_{gp} + Q_{cai} + Q_{cao} = 0; \quad u = 0, \quad v = 0 \tag{13}$$

For the porous absorber outside surface

$$x = h_{po}, \quad k_m A_P \frac{dT_p}{dx} = \delta\eta_p G_{sun} A_p + Q_{gp} + Q_{apo}$$

$$u|_{x=h_{po}^-} = u|_{x=h_{po}^+}, \quad v|_{x=h_{po}^-} = v|_{x=h_{po}^+}, \quad p|_{x=h_{po}^-} = p|_{x=h_{po}^+},$$

$$\mu_m\left(\frac{\partial u_d}{\partial y} + \frac{\partial v_d}{\partial x}\right)\Big|_{x=h_{po}^-} = \mu\left(\frac{\partial u}{\partial y} + \frac{\partial v}{\partial x}\right)\Big|_{x=h_{po}^+} \tag{14}$$

For the separation type porous absorber inside surface

$$x = h_{pi}, \quad K_m A_P \frac{dT_p}{dx} = Q_{pw} + Q_{api},$$

$$u|_{x=h_{pi}^-} = u|_{x=h_{pi}^+}, \quad v|_{x=h_{pi}^-} = v|_{x=h_{pi}^+}, \quad p|_{x=h_{pi}^-} = p|_{x=h_{pi}^+}, \tag{15}$$

$$\mu_m\left(\frac{\partial u_d}{\partial y} + \frac{\partial v_d}{\partial x}\right)\Big|_{x=h_{pi}^+} = \mu\left(\frac{\partial u}{\partial y} + \frac{\partial v}{\partial x}\right)\Big|_{x=h_{pi}^-}$$

For the inside surface of the contact type porous absorber, the boundary condition of Eq. (15) is omitted.

For the thermal storage wall inside surface

$$k_w A_{wall}\frac{\partial T_{wall}}{\partial x} = h_{wi}A_{wall}(T_{room} - T_{wall}); \quad u = 0, \quad v = 0 \tag{16}$$

For the heated room

$$(\rho c V)\frac{\partial T_{room}}{\partial \tau} = h_{wi}A_{wall}(T_{wall} - T_{room}) + Q_{wr} \tag{17}$$

3. Numerical procedure

For the present study, the governing Eqs. (1)–(12) together with the boundary conditions mentioned above were solved with the SIMPLER method. The computer code based on the mathematical formulation discussed earlier and the SIMPLER method is validated for various cases publish in the literature [14]. The control-volume formulation utilized in this method ensures continuity of the convective and diffusive fluxes as well as overall momentum and energy conservation. The harmonic mean formulation was used to handle abrupt variations in the thermal physical properties, such as the permeability and thermal conductivity, across the interface, for example, at the porous/fluid layer interface. This ensured the continuity of convective and diffusive flues across the interface without requiring the use of an excessively fine grid structure.

Non-uniform mesh sizes were used for the numerical computation. The grid in horizontal direction was uniformly distributed. In vertical direction, finer mesh sizes were taken within the porous absorber. To test the grid independence, two different grid sizes had been employed in the present study. The numbers of grid considered were 108×88 and 128×108 which correspond to a uniform. Therefore, to achieve favorable CPU computation time in the simulation, a grid of 108×88 had been chosen for this study.

As far as the unsteady-state numerical calculations, the time step was concerned and several values of $\Delta\tau$ had been examined for the grid chosen. For example, It had been found that the maximum deviation between the results using $\Delta\tau = 30$ s and $\Delta\ \tau = 45$ s was only 2.5%. Hence, the time step of $\Delta\tau = 45$ s together with the grid size of 108×88 were used for the unsteady-state numerical calculations performed in this study.

The porous layer made of Quartzite and the thermal storage wall made of Concrete were chosen in the simulation. To analyze the effect of porous materials on the heating performance of the composite wall, Quartzite and Marble were chosen as sample. Their physical properties are:

Quartzite [15]: $\rho = 2635$ kg/m^3, $c = 0.732$ kJ/(kg K), $k_p = 5.17$ W/(m K).
Concrete [15]: $\rho = 2243$ kg/m^3, $c = 0.837$ kJ/(kg K), $k_s = 1.5$ W/(m K).
Marble [15]: $\rho = 2650$ kg/m^3, $c = 0.840$ kJ/(kg K), $k_s = 2.7$ W/(m K).

The volume of the selected heated room is 18 m^3, in which the air is heated by the composite wall. The composite solar wall dimensions are 0.24 m wide, 2.5 m high. The width of the porous layer is 0.05 m.

4. Experiment procedure

The experimental setup for the two types of composite solar wall with porous absorber could be established as Fig. 1. The porous absorber with marble diameter $d_m =$ 1–2 cm and absorber porosity $\theta = 0.2$–0.3, $d_m = 1$–2 cm and $\theta = 0.5$–0.6 as well as quartzite diameter $d_q = 1$–2 cm and absorber porosity $\theta = 0.5$–0.6 are selected respectively in the two types of composite solar wall. The thermal insulation is laid between the different types of the porous absorber. The temperature is measured with thermocouples, monitored by a digital voltage reader. Thermocouples are mounted on the outside surface and the inside surface of the porous absorber, the inside surface of the thermal storage wall, and in the middle of the heating room, respectively. The ambient temperature is measured with a digital thermometer. The airflow speed is measured with an anemometer. Solar radiation is measured with an actinography. All measurements are repeated more than three times for each experimental data used. The above experimental procedure for the solar composite wall with porous absorber is given and can be carried out to validate the numerical results.

5. Results and discussion

To analyze the effects of the porous absorber on the temperature distribution and gas flow in the composite solar wall, and to discuss the influences of the position of porous absorber in composite wall, the particle size and the porosity within the porous absorber and the material of porous absorber on the heated room temperature, we made the numerical calculation for the present model. The temperature unit in the Isotherm figures is °C. The results are analyzed as follows:

Observing Fig. 2, we can find that during the heating time, the surface of the porous absorber has higher temperature comparatively and the solar energy absorbed by the porous layer in the heating system was used to increase the air temperature in the heated room and thermal storage wall. In contrast, when the sun is no shining, the temperature of the thermal storage wall is higher and heat stored in the massive wall releases to raise the air temperature in the heated room. The air temperature change in the heated room is the same as the inside surface of thermal storage wall.

As shown in Figs. 3 and 4, in the separation type porous absorber composite wall, the air temperature near the bottom is lower, in contrast, the air temperature near the up of the heating wall is higher, and the temperature gets to rise from the bottom to the top. The heat exchanges between

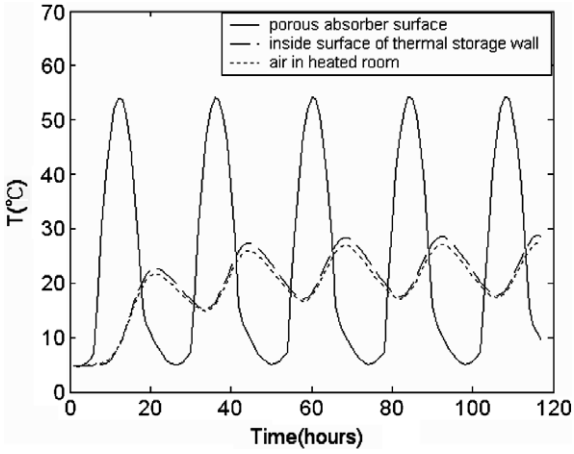

Fig. 2. Comparison of predicted values of temperature among outside surface of porous absorber, air in heated room and inside surface of thermal storage wall in contact type passive solar composite wall with porous absorber ($d_p = 1$ cm, $\theta = 0.55$).

the porous absorber and the thermal storage wall in convective heat transfer and thermal radiation, so the temperature of wall rises and the air in the room is heated. In contact type porous absorber composite wall, the solar irradiation absorbed by porous layer is used to heat the south wall in thermal conduction and convective heat transfer. The comparison of the flow and temperature field inside the composite solar wall made among at 12:00, at 16:00, at 19:00 and at 24:00 can show that the peak temperature within the composite wall moves in versus time. During the solar radiation such as at 12:00 and at 16:00 in the afternoon, the convective heat exchange within the porous absorber is intensified comparatively. In contrast, when the sun is not shining such as at 19:00 and 24:00, the convection is thus strongly reduced and the outside surface temperature of the porous layer is much more below that of the inside surface temperature of the porous layer, so the convective heat exchange and the radiation exchange between the composite solar wall and the ambient decreases and the heat loses of the heating system is strongly reduced; as the excess heat is stored within the porous absorber during solar radiation and there is stratification in the porous layer, the inside surface temperature of the porous absorber is higher comparatively. Therefore, when the sun is not shining, the porous layer servers as semi-thermal insulator.

In comparison with the separation type composite wall, it can be seen that in the contact type composite wall, the inside surface temperature of the thermal storage wall is higher, and the temperature difference between the outside surface of the porous absorber and the inside surface of the thermal storage wall is lower when the sun is shining such as at 12:00 and at 16:00, so more heat is available for heating; when no solar irradiation is available such as at 19:00 and 24:00, the temperature difference is higher and the heat loss from the heated room to the ambient decreases.

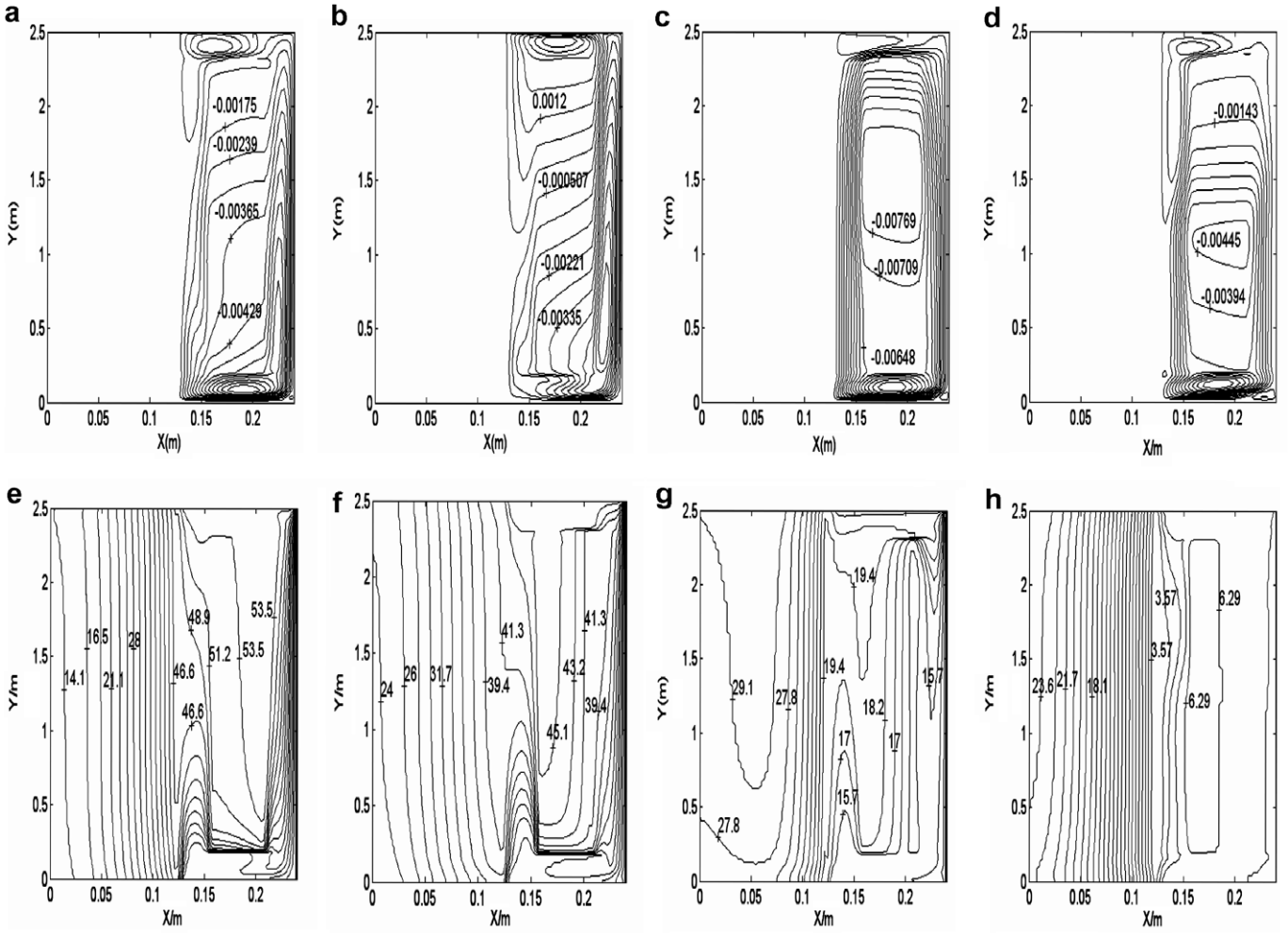

Fig. 3. Development of fluid and temperature (°C) field with time for the separated type passive solar composite wall with porous absorber ($d_p = 1$ cm, $\theta = 0.55$): (a) streamlines at 12:00 noon; (b) streamlines at 16:00 in the afternoon; (c) streamlines at 19:00 in the evening; (d) streamlines at 24:00; (e) isotherms at 12:00 noon; (f) isotherms at 16:00 in the afternoon; (g) isotherms at 19:00 in the evening and (h) isotherms at 24:00.

From Figs. 5 and 6, it can be seen that, in contrast to the contact type composite wall with porous absorber, there exists wide range of temperature in the separation type. The insufficiency heating may happen in the composite wall without porous absorber. In the separation type composite wall with a porous absorber, at particle diameter of 1 cm, the porosity of porous absorber changes from 0.2 to 0.55, and at the porosity of 0.55, the particle diameter changes from 0.22 cm to 1 cm, the air temperature of the heated room rises. In the contact type composite wall, at particle diameter of 1 cm, with the porosity of porous absorber changing from 0.2 to 0.35 and 0.55, the temperature of porous absorber at depth of 4.9 cm increases. However, there is higher temperature within the porous absorber of 0.35 porosity in contrast to the porous absorber of 0.55 porosity as shown in Fig. 7. The heat transfer within porous absorber is mainly in thermal conduction and convection. With the increase of the particle diameter and porosity, the convective heat exchange in porous medial is intensified, but heat exchange in thermal conduction decreases. The particle size, porosity within porous absorber should be chosen reasonably, so the more heat absorbed by porous medial is transferred into the heated room.

Fig. 8 shows that the air temperature in the heated room of different porous absorber materials changes versus time for Quartzite and Marble, which have the typical characteristics for porous absorber. It is clear that the air temperature in heated room varies more greatly versus time and is higher relatively in the periods of the solar radiation when Quartzite with higher thermal conductivity is used for porous absorber. However, when the sun is not shining, the air temperature in heated room with Marble porous absorber which has lower thermal conductivity is higher. Therefore, there is an important influence of thermal conductivity of porous absorber on the heating.

Besides, the top air temperature inside the room is a little above 20 °C in the simulation, thus the particle size and the porosity within the porous absorber and the material of porous absorber should be chosen properly to provide comfort air temperature in the heated room. In contrast to the air temperature in the room with the porous composite wall presented in the literature [5], the air temperature

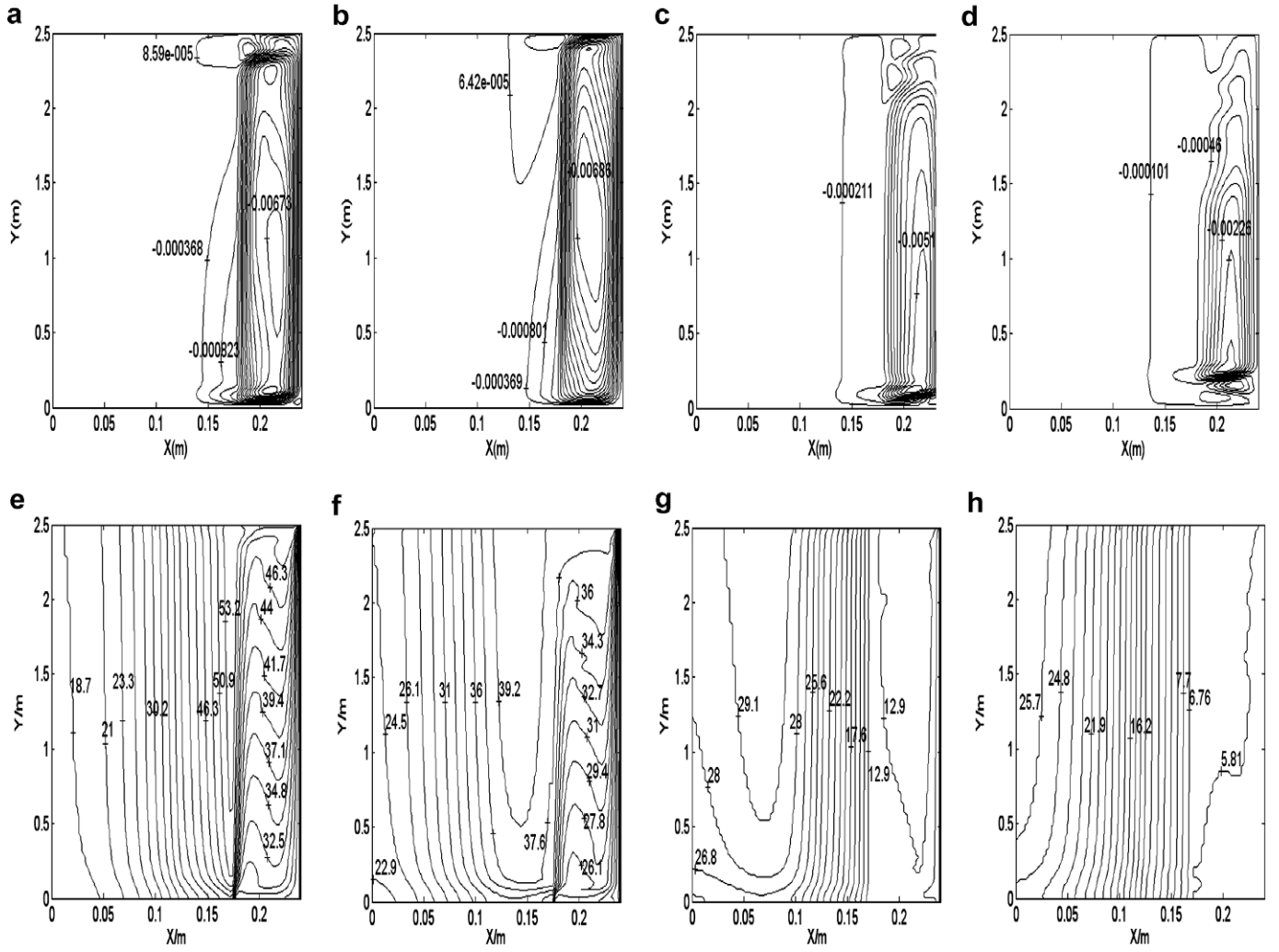

Fig. 4. Development of fluid and temperature (°C) field with time for the contact type passive solar composite wall with porous absorber ($d_p = 1$ cm, $\theta = 0.55$): (a) streamlines at 12:00 noon; (b) streamlines at 16:00 in the afternoon; (c) streamlines at 19:00 in the evening; (d) streamlines at 24:00; (e) isotherms at 12:00 noon; (f) isotherms at 16:00 in the afternoon; (g) isotherms at 19:00 in the evening and (h) isotherms at 24:00.

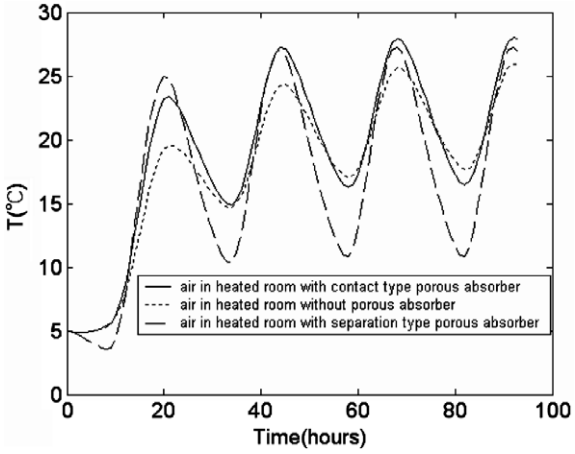

Fig. 5. Hourly values of air temperature change versus time in heated room with contact porous absorber ($d_p = 1$ cm, $\theta = 0.55$), in heated room with separation type porous absorber ($d_p = 1$ cm, $\theta = 0.55$) and in heated room with absorber of no porous layer.

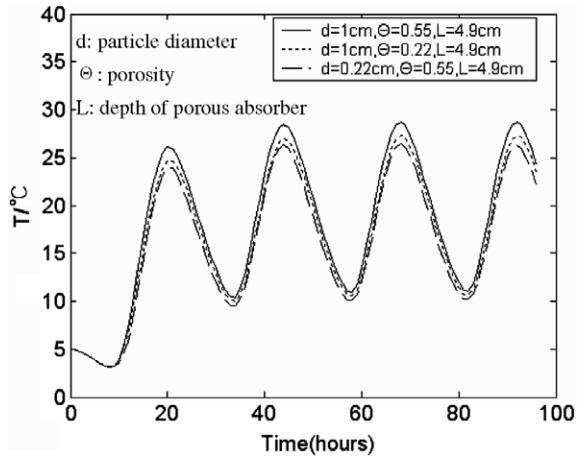

Fig. 6. Temperature of porous absorber change versus time for different diameters and porosities of porous medium in separation type porous absorber.

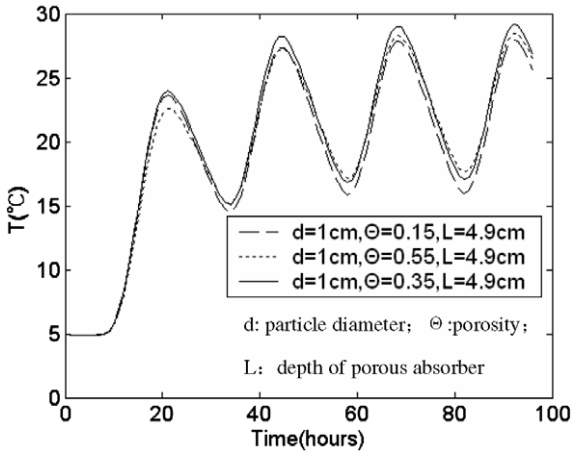

Fig. 7. Temperature of porous absorber change versus time for different porosities of porous layer in contact type porous absorber.

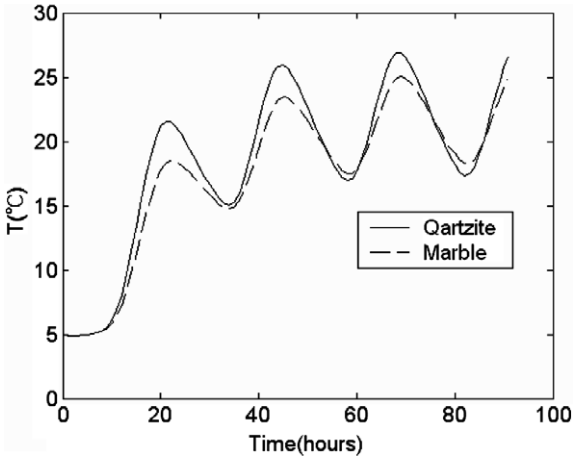

Fig. 8. Hourly values of air temperature in heated room change versus time for various material of porous absorber ($d_p = 1$ cm, $\theta = 0.55$).

rises more slowly and the top temperature postpones appearing in the heated room with the separation type or the contact type of the porous composite wall shown in Fig. 1.

6. Conclusions

A numerical model has been developed to study the effects of the porous absorber on the temperature distribute and airflow in the two types of the composite solar wall. From above discussion, we have found that the possibility of insufficient in the heating system decreases greatly and the thermal resistance of composite wall increases at night or on a cloudy day, if a convective porous layer is used as a solar absorber inside composite wall. The excess heat is stored and a temperature gradient exists within porous absorber. The layer can work as a semi-thermal insulator when solar radiation is not available. The influence of permeability within the porous absorber, the material of porous absorber and the position of the porous absorber in the composite wall on the heated room temperature is significant. In contrast to the separation type composite wall with porous absorber, there exits higher average temperature in the contact composite wall. Therefore, the particle sizes and porosity within the porous absorber, the material of porous absorber and the position of the porous absorber in the composite wall should be chosen properly to avoid the occurrence of the overheating and the no reaching the heating requirements when the solar shining is available.

Acknowledgements

The current work is financially supported by the National Natural Science Foundation of China (No. 50376015) and Shanghai Education Committee Foundation.

References

[1] F. Trombe, Maisons solaires, Techniques de l' IngTenieur 3 (1974) C777.
[2] R. Ben Yedder, E. Bilgen, Natural convection and conduction in Trombe wall systems, International Journal of Heat and Mass Transfer 34 (4/5) (1991) 1237.
[3] Z. Zrikem, E. Bilgen, Theoretical study of a composite Trombe–Michel wall solar collector system, Solar Energy 39 (1987) 409–429.
[4] Z.-G. DU, E. Bilgen, Natural convection in composite wall collectors with porous absorber, Solar Energy 45 (6) (1990) 325–332.
[5] Wei Chen, Wei Liu, Numerical analysis of heat transfer in a composite wall solar-collector system with a porous absorber, Applied Energy 78 (6) (2004) 137–149.
[6] M. Mbaye, E. Bilgen, Natural convection and conduction in porous wall: solar collector systems without vents, Journal of Solar Energy Engineering, Transactions of ASME 114 (February) (1992) 40–46.
[7] D.A.S. Rees, The onset of Dary–Brinkman convection in a porous layer: an asymptotic analysis, International Journal of Heat and Mass Transfer 45 (2002) 2213–2220.
[8] Ergun, Fluid flow through packed columns, Chemical Engineering Progress 48 (1952) 89–92.
[9] C. Beckermann, S. Ramadhyani, R. Viskanta, Natural convection flow and heat transfer between a fluid layer and a porous layer inside a rectangular enclosure, Journal of Heat Transfer 109 (May) (1987).
[10] G. Neale, W. Nader, Practical significance of Brinkman's extension of Darcy's law, Canadian Journal of Chemical Engineering 53 (1974) 475–478.
[11] Falin Chen, C.F. Chen, Convection in superposed fluid and porous layers, Journal of Fluid Mechnics 234 (1992) 97–119.
[12] Wei Chen, Wei Liu, Bingcheng Liu, Numerical and experimental analysis of heat and moisture content transfer in a lean-to greenhouse, Energy and Buildings 38 (2006) 99–104.
[13] Wei Chen, Wei Liu, Numerical simulation of the airflow and temperature distribution in a lean-to greenhouse, Renewable Energy 31 (2006) 401–568.
[14] Tao Wen-Quan, Numerical Heat Transfer, second ed., Xi'an Jiaotong University Press, 2001, pp. 385–329.
[15] Ma Qing-Fang, Practical thermal physical property handbook, The Chinese Agriculture Mechanics Press, 1986, pp.701–710.